



Temperature Distribution Analysis in a Cold Room with Heated Carpets

B T I ghobrial¹, A M M abdalla², K F Megala³, A R abohabsa⁴

Mechanical power department, Faculty of Engineering, Helwan University, Cairo 11817, Egypt



CrossMark

Abstract

A practical experiment to analyse the distribution of air in terms of temperature ratios in a room with heated carpets and the influence on the surrounding environment is performed. Some countries with very low temperatures and high density values require one of the heating procedures to provide human comfort conditions (temperature about 25 °C, humidity around 50%). In this study, it is realistically explored how different types of heated carpets of varying weaves affect the temperature distribution inside the room. Experiments were also conducted at a heat flux value of 120 W/m², with measurement locations above, near, and distant from the heated surface, as well as at different times (15 and 25 minutes) and height ratios. The results show that the values of temperature ratio of full piled carpet are (1.035568, and 1.036934) far from the carpet, and the values are (1.036592, and 1.038641) near the carpet; respectively at 15 and 25 minutes, height ratio of 0.0625 and 120 W/m². The values of the temperature ratio of partially piled carpet increase to (1.04146 and 1.04351) near the carpet, compared to the full piled carpet under the same conditions.

This is due to the presence of spaces (areas without pile) on the surface of the partially piled carpet, allowing for easier heat transfer compared to the full piled carpet leads to an increase in the temperature values.

The partially piled carpet has a greater impact on the room to be heated by using hot carpets, as it has the highest temperature values and the lowest density values. Empirical correlations have been developed depending on the study operating conditions.

Keywords: Temperature ratio, Heated carpet, Air distribution.

1. Introduction

The winter season is one of the most difficult things to happen in many areas throughout the world when temperatures decrease most of the year. These issues are unfamiliar in the countries and sectors of East and North Africa, as well as Northern Europe, North America, and East Asian countries.

Heating historic buildings always has an effect on the indoor air temperature and humidity, which are critical for conserving historic interiors. Because modern rehabilitation prioritises such interiors, local heating was chosen as the approach of choice to prevent potential injury while providing high levels of occupant comfort.

Due to installation concerns, system use, and especially system operation, such heating technologies as radiant flooring might upset the delicate comfort-conservation balance. The underfloor radiant heating installed as part of a recent repair has demonstrated to efficiently sustain maximum occupant comfort (Categories I-II) up to a height of 2 m off the floor[1], with no immediate impact on the dome mural paintings, which are at a far higher elevation.

In a space where people would be spending a lot of time, a comfortable thermal climate was critical.

Because heating a home consumes a lot of energy, an energy-efficient heating system will be required. Then, by combining a heat pump with underfloor heating, it was possible to achieve both thermal comfort and energy savings. The survey was conducted in Nagano Prefecture, Japan, on a separate house. On average, the temperature outside was 4.2°C. In their investigation, the indoor thermal environment was analysed, the operating performance of the heat pump was evaluated, and the heat load was calculated using two-dimensional analysis[2]. Their research offered the thermal modeling and best design of an underfloor heating system. Analytical modeling in conjunction with experimental data was used to determine the rate of heat transfer and temperature distribution in the system under investigation. Following thermal modeling, four design elements were considered: tube length, tube radius, water mass flow rate, and the number of panels. Both algorithms achieved convergence with a 0.2 percent difference.

According to the results of the optimization to design underfloor heating systems, there should be 13 underfloor heating panels, each with an inside radius of 7 mm and an overall length of 80 meters. Water should flow at a rate of 0.503 kg/s through these tubes.

*Corresponding author e-mail: Eng.basemgh15@m-eng.helwan.edu.eg

Receive Date: 06 August 2022, Revise Date: 09 September 2022, Accept Date: 28 September 2022

DOI: 10.21608/EJCHEM.2022.153408.6645

©2022 National Information and Documentation Center (NIDOC)

A sensitivity analysis is also performed to assess how the design parameters of the underfloor heating system affect the best total annual cost, rate of heat transfer, and panel temperature. The results showed that increasing the design parameters increased both the annual total cost and the rate of heat transmission[3]. Convection and radiative heat transfer were modeled to achieve an appropriate level of interior temperature. The findings came from a pilot study that comprised the construction of an energy-efficient dwelling west of Algiers. The primary goal was to conduct a numerical simulation to investigate how surface radiosity affected the temperature profile of the inside air, as well as how the temperature of the heat-transfer fluid running in the floor heating system affected those two variables.

The model was validated using experimental data from the pilothouse obtained under identical meteorological circumstances as published in the literature. It was determined that increasing the temperature of the heating transfer fluid from 30 to 50°C resulted in a 15.1°C rise in room temperature measured at a height of 50 cm. The air temperature remained stable with a slight change after 72 hours of heating [4,13].

Another study looked into under-floor water heating systems and wood flooring. Wood is a very sensitive substance that responds to its surroundings. Because of this, it was vital to select a wood that matched the standards for installation as flooring in conjunction with underfloor heating systems. Furthermore, it was critical to adhere to the technical requirements for the installation of wooden flooring in conjunction with underfloor heating systems throughout the entire life cycle of the wood flooring, as well as the conditions for storage and installation of the flooring at the construction site under acceptable climatic conditions[5].

According to the International Energy Agency, buildings are the world's largest energy consumer, accounting for more than one-third of total greenhouse gas emissions in 2013. Renewable energy sources such as solar can meet a portion or all of the energy needs of buildings. Solar thermal collectors are used in their study to provide hot water for an underfloor heating system in a building. To better understand how solar-powered underfloor heating systems work in different climates, three Iranian towns with distinct climatic circumstances were chosen: Tabriz, Tehran, and Kish Island [6,17]. Incorporating phase change materials (PCM) into various architectural components increases thermal mass, cutting energy consumption and moving peak load. The benefits of PCM inclusion in walls, ceilings, and in conjunction with PCM underfloor heating systems were illustrated using two types of PCMs.

Using lower melting point PCM in the walls and ceiling provided the requisite building comfort, while using higher melting point PCM with the underfloor heating system allowed for significant peak load shifting. Two comparable huts built on the Tamaki Campus of the University of Auckland (New Zealand) were modeled using the application Energy Plus. The simulation's results were validated using experimental data from two office buildings[7,14].

A quarter-scale insulated prototype of an underfloor heating system was constructed and tested utilising coconut oil as a new bio-based phase change material (PCM). There were two cases investigated. In the first experiment, the PCM was placed in an Aluminum container above an electrical heater, and its adaption to the floor was studied. The second case acted as a control test in the absence of PCM plates. Winter heating demands can be decreased while maintaining household thermal comfort thanks to the adaptability of the underfloor system with PCM. An economic study based on current electricity shifts was then used to estimate the system's capacity for peak load shifting [8,15].

The analysis above revealed that underfloor heating is one of the methods for warming the rooms. However, there is little information in the literature about the thermal distribution of the novel method of deeply heating the floor using various heated carpets.

In this study, the effect of different heated carpets inside a room on air temperatures and consequently air motion to achieve human comfort levels has been studied. Two heated surfaces are used in this experiment. The Two heated surfaces are two distinct carpets heated by a flat electrical heater. Different pile densities are used in these carpets. Different operating conditions are conducted varying: room temperature (20 °C), The heat source (120 W/m²), the measurement places above, near, and far from the heated surface, and transient state (15: 25 minutes).The temperature measurements are carried out in the form of a grid at 42 points inside the room. In graphs and contours, the temperature distribution is displayed. Empirical correlations have been developed depending on the study operating conditions

Experimental Apparatus Descriptions

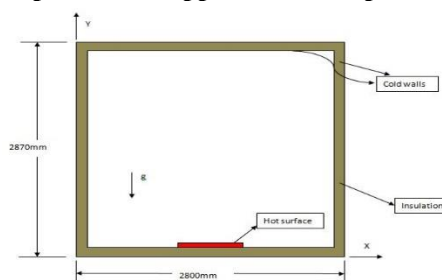


Figure 1. Schematic diagram of the room

The test facility consists of a room with dimensions of (280, 287, and 160 cm) as shown in Figure 1. As a heat source, the room has a heated carpet facility as shown in Fig. 2. The walls of the room are insulated. Carpet, an Aluminum plate, an electric heater, and wool insulation make up the heated carpet facility. The carpet used is made of synthetic fiber. Two carpets that have been thoroughly tested are employed. Carpet 1 or full-pilled carpet is the first carpet. The second carpet is referred to as carpet 2 or partially pilled carpet as shown in Fig. 3.

The room was instrumented with 42 thermocouples as shown in Figure 4. The temperature of the air is measured above, near, and distant from the heated surface using thermocouples that are linked to Arduino cards that receive the signals and transmit the readings to computers. To begin, the indoor air temperatures are managed by the air conditioner to be in the 20 °C range prior to turning on the heater. When the room becomes cold, the air conditioning is turned off, and the electric heater starts working at various periods under controlled exterior operating conditions.

The effort attempts to develop additional possible solutions for the heating system employed by using different types of heated carpets, as well as how to affect the distribution of room temperatures under the influence of varying pile densities over the carpet surface.



a. Heated carpet



b. compare between the cross section area for two carpet

Figure 2. Heated carpet facility, and the cross section area



a) full pilled carpet (gray& black colours).



b) partially pilled carpet (gray & reddish mauve colours).

Figure 3. Experimental carpets; a) partially pilled carpet (gray& black), and b) full pilled carpet (gray & reddish mauve).

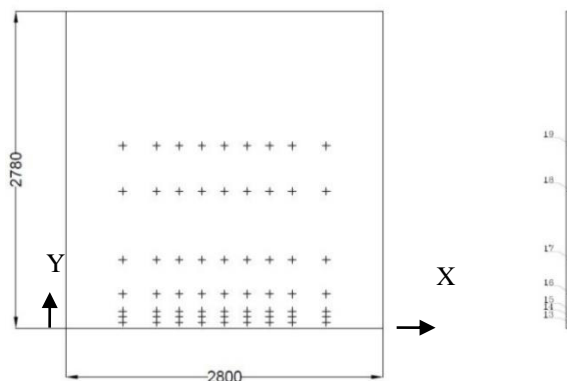


Figure 4. Test section for Thermocouple locations(mm)

A precise method of estimating the uncertainty in the experimental results has been described by Holman (1978). *Holman, J.P., 1978. Experimental methods for engineers. McGraw-Hill, New York, NY*

the method is based on a careful specification of the uncertainties in the various primary experimental measurements. The result M is given as a function of the variables (x, y, z,t), thus:

$$M = f(x, y, z,t) \quad (1)$$

If e_M is the uncertainty in the result, and $e_x, e_y, e_z, ,e_t$ are the uncertainties in the variables. If the uncertainties in the variables are all known, then the uncertainty in the result is defined as:

The error analysis considered in the results obtained for the sample in Table 2 is obtained and presented in the following sections.

$$Ra = \frac{g \beta (T_s - T_\infty) L^3}{\nu^2} \quad (3)$$

$$\partial Ra / \partial I = 0, \partial Ra / \partial T_{inf} = -4.001E+10, \partial Ra / \partial T_s = 1.930E+10, \text{ and } \partial Ra / \partial Volt = 0,$$

$$e_M = \left[\left(\frac{\partial M}{\partial x} \cdot e_x \right)^2 + \left(\frac{\partial M}{\partial y} \cdot e_y \right)^2 + \left(\frac{\partial M}{\partial z} \cdot e_z \right)^2 + \dots + \left(\frac{\partial M}{\partial t} \cdot e_t \right)^2 \right]^{\frac{1}{2}} \quad (2)$$

Table 2 Uncertainty values of experiment and calculated variables

Parameters	T_s	T_{inf}	T_f	Volt	I_{curr}	ρ	S	q''	Ra
Degree of uncertainty	± 0.1	± 0.1	± 0.070	± 0.06	± 0.00063	± 0.000411	± 0.3449	± 0.03564	$\pm 4.442E+09$
y	$^{\circ}C$	$^{\circ}C$	$^{\circ}C$	volt	Amp	kg/m^3	$kJ/kg K$	W/m^2	$[-]$

Where: T_s : surface temperature, T_{inf} : temperature of the air, T_f : film temperature (average temperature between the surface and the room air temperature), I_{curr} : electrical current, ρ : density, S: entropy, q'' : heat flux, and Ra: Rayleigh number.

Results

The temperature ratio (T_r) means the temperature at each point relative to the average room temperature before operation (before turn on the heater), and the height ratio means the height at the measurement point in relation to the room total height (160 cm). The effect of changing the temperature ratio with the height ratio is studied for the full piled carpet, and the partially piled carpet. With changing the value of the heat load, i.e., the rate of heat transfer by controlling the voltage regulator, experiments were carried out at values of 9 and $120 W/m^2$.

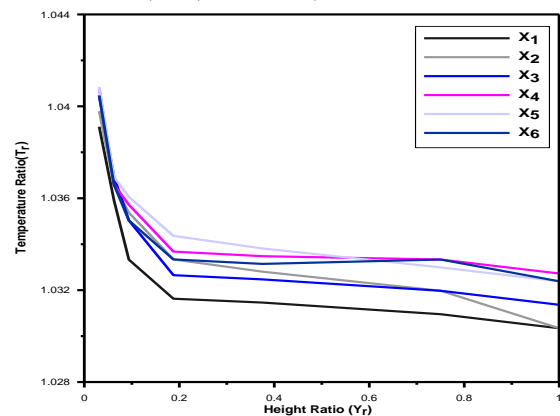
Figure 5 illustrates the relationship between (T_r) and (Y_r) of the first heated carpet, at a heat load of $120 W/m^2$, during measurement times of (25, and 35 minutes), and at various measurement locations ($X_1, X_2, X_3, X_4, X_5,$ and X_6).

The temperature ratio trend is consistent throughout all operating conditions, as shown in this graph. The temperature ratio is highest near the wall and drops as you get further away from it.

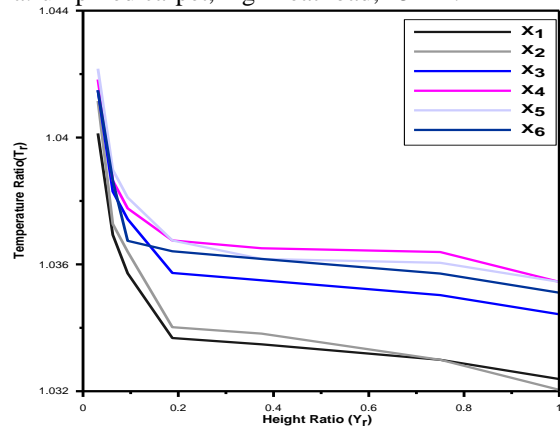
To trace the values of (T_r) at the locations of (X_2 and X_4), times of (15, and 25 minutes) and height ratio of ($Y_r \approx 0.03125$), Figs.(5a-b) will be used. The values of (T_r) are (1.03877, and 1.04081) at X_2 , while the values of (T_r) at location (X_4) are (1.040471, and 1.041491); respectively.

Figure(6) shows the relationship between (T_r) and (Y_r), for the partially piled carpet, at the heat load of $120 W/m^2$, measurement time of (25, and 35 minutes), measurement locations of ($X_1, X_2, X_3, X_4, X_5,$ and X_6). Figure(6a) shows the experiment is carried out after 15 minutes. The value of (T_r) increases to 1.045 compared to the full piled carpet which the value of (T_r) is 1.0408 under the same conditions. This is due to the presence of spaces (areas without pile) on the surface of the carpet (2), allowing for easier heat transfer compared to the full piled carpet leads to an increase in the temperature values.

Figure(6b) shows the experiment is carried out after 25 minutes. This figure shows a significant increase in the values of (T_r) compared to Figure(6a). Figures(6a-b) show the trace value of (T_r), at the measurement locations of (X_2 and X_4) and different times of (25, and 35 minutes) at ($Y_r = 0.0625$).

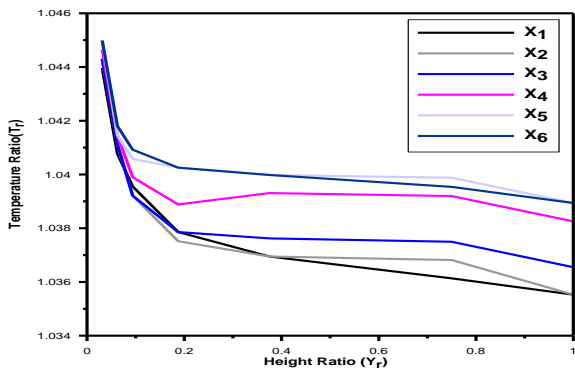


a. full piled carpet, high heat load, 15min.

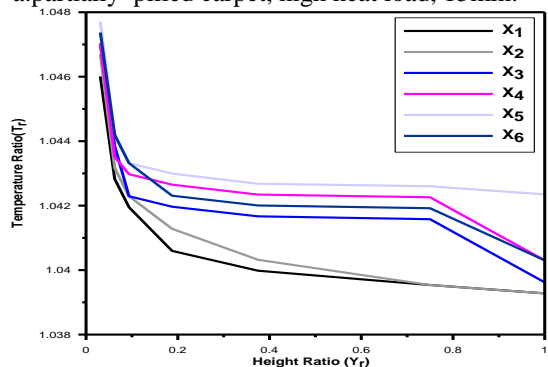


b. full piled carpet, high heat load, 25min.

Figure 5. Temperature ratio of full piled carpet, at high heat load, at different time



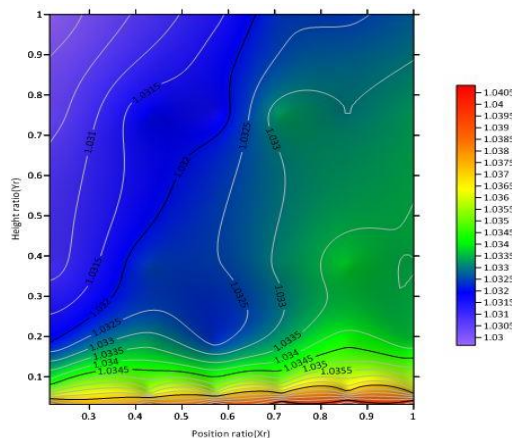
a. partially piled carpet, high heat load, 15min.



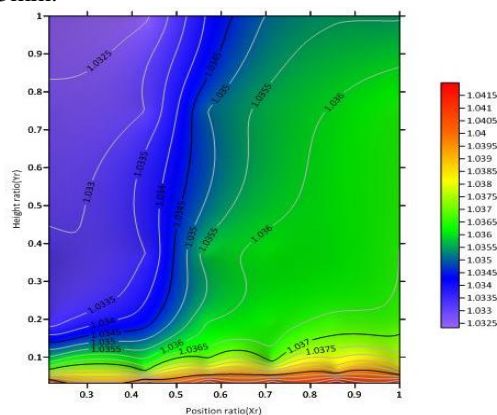
b. partially piled carpet, high heat load, 25min.

Figure 6. Temperature ratio of partially piled carpet, at high heat load, at different time

As shown in Figs. 7 and 8, the thermal distribution contour in the room with full piled carpet and partially piled carpet. These figures show four distinct areas: the first region locates over the hot surface (red color), near the hot surface (yellow color), far from the hot surface (green color) which less exposure to radiation and convection heat transfer, and second region is close to the room borders, which is characterised by the cold environment (blue color). The temperature ratio distribution in the room with full piled carpet at various periods and with a lower heat load is shown in Fig. 7. The temperature of indoor air increases gradually with time as shown in the legend of Figs.7(a-b). Fig. 8 shows the temperature ratio distribution in the room equipped with partially piled carpet at different times and lower heat load. It shows higher temperature values inside the room compared to the room with full piled carpet. This is due to the fact that the insulation layers (piles) in the partially piled carpet did not completely cover the surface, increasing the amount of heat transfer from the heated carpet to the areas around it in the room.

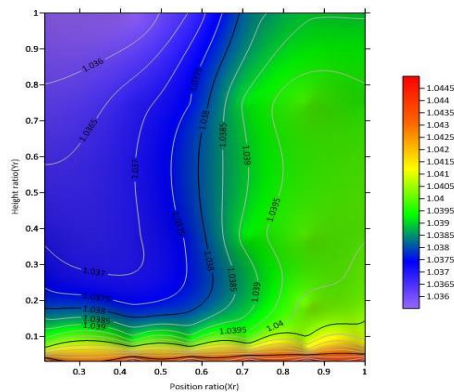


at 15min.

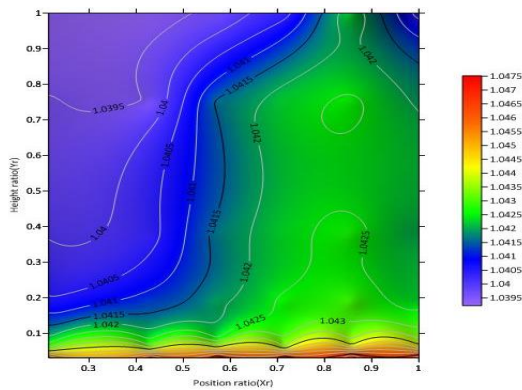


at 25min.

Figure 7. Contour of T_r of full piled carpet, at a high heat flux and different times



at 15min.



at 25min.

Figure 8. Contour of T_r of partially filled carpet, at a high heat flux and different times

Experimental correlations of temperature ratio for a room with heated carpets

The temperature ratio ($T_r = \frac{T}{T_i}$) is functions of streamwise (position) ratio ($X_r = X/W$), height ratio ($Y_r = Y/H$), time ratio ($t^* = \text{time}/35$), heat flux ratio ($q^* = q''/120$), and carpet type. Therefore, the relationship of temperature ratio is written as follows:

$$T_r = f\left(\frac{X}{W}, \frac{Y}{H}, t^*, q^*, \text{carpet type}\right)$$

The relationship between temperature ratio (T_r) and streamwise ratio (X/W). Regression analysis is used to create a fitting, then the relationship is as follows:

$$T_r = 1.025 * X_r^{0.003} \tag{4}$$

The constant 1.025 in Eq. [4] will be a function of other parameter i.e., height ratio (Y_r). So $\frac{T_r}{X_r^{0.003}} = 1.025$ is plotted as a function of height ratio (Y_r). By using the regression analysis, the relationship is:

$$\frac{T_r}{X_r^{0.003}} = 1.028 Y_r^{-0.002} \tag{5}$$

Further, the constant 1.028 in Eq. [5] will be a function of other parameter i.e., time ratio (t^*).

So $\frac{\frac{T_r}{X_r^{0.003}}}{Y_r^{-0.002}} = 1.028$ is plotted as a function of time ratio (t^*). By using the regression analysis, the relationship is:

$$\frac{\frac{T_r}{X_r^{0.003}}}{Y_r^{-0.002}} = 1.032 t^{*0.003} \tag{6}$$

Also, the constant 1.032 in Eq. [6] will be a function of another parameter i.e., heat flux ratio (q^*).

So $\frac{\frac{\frac{T_r}{X_r^{0.003}}}{Y_r^{-0.002}}}{t^{*0.003}} = 1.032$ is plotted as a function of heat flux ratio (q^*). By using the regression analysis, the relationship is:

$$\frac{\frac{\frac{T_r}{X_r^{0.003}}}{Y_r^{-0.002}}}{t^{*0.003}} = 1.039 q^{*0.004} \tag{7}$$

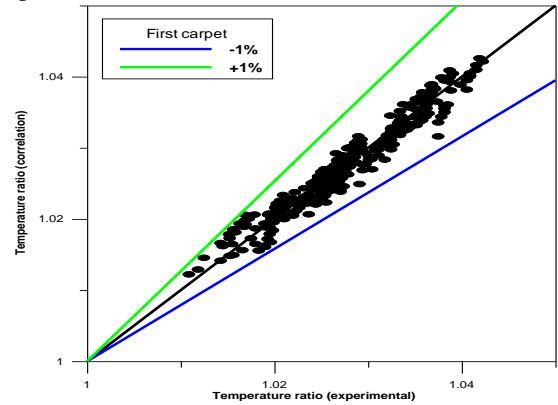
After rearranging Eq. [7], the final correlation of temperature ratio for full filled carpet is:

$$T_r = 1.039 X_r^{0.003} Y_r^{-0.002} t^{*0.003} q^{*0.004} \tag{8}$$

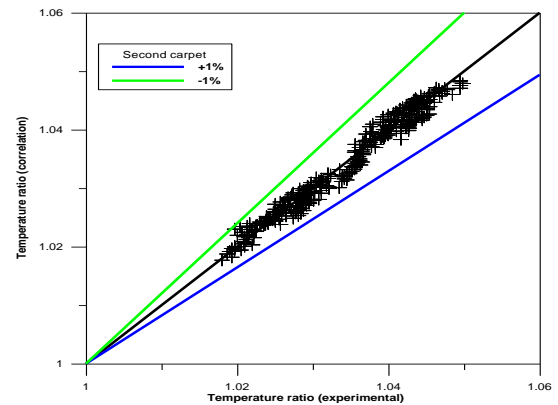
A similar procedure is employed for partially filled carpet. The correlation of temperature ratio for partially filled carpet is as follow:

$$(T_r) = 1.0422 * X_r^{0.00149} * Y_r^{-0.0017267} * t^{*0.00379968} * q^{*0.0054313} \tag{9}$$

The deviation between experimental and predicted data from correlation for full and partially filled carpet, +1% and -1% for both cases.



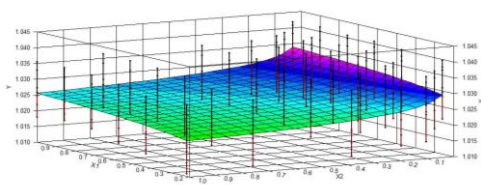
a. Full filled carpet



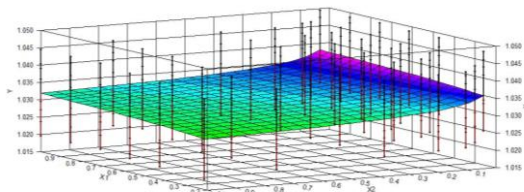
b. Partially filled carpet

Figure 9. Comparison of the experimental data and predicted correlation : full and partially filled carpet

Figure(10) shows the three-dimensional effect of temperatures inside the room, width ratio values (X_1), height ratio values (X_2), and temperature ratio values (Y) together. The temperature ratio values increase through the right part of the drawing, which represents the upper part of the hot carpet's surface and the lowest point of the room's height.



a) Full pilled carpet, high heat load



b) Partially pilled carpet, high heat load

Figure 10. three-dimensional effect of temperatures inside the room, for two models

Conclusion

An experimental test device was set up to determine the best heat distribution for a room heating system. Temperatures were measured at 42 points during the experiment using different types of heated carpets to calculate the temperature ratio (T_r). The effect of room temperature, heat flow, different times (15, and 25 minutes), and different locations above the hot surface, near and far from it, are studied.

From the experimental results, the following conclusions can be drawn:

1. The values of (T_r), for full pilled carpet after 15 minutes and $Y_r=0.0625$, at heat load 120W/m^2 were (1.03523, 1.03557, 1.03557, 1.03659, 1.03693, and 1.03659), at (X_1, X_2, X_3, X_4, X_5 , and X_6).
2. The values of (T_r), for partially pilled carpet after 15 minutes and $Y_r=0.0625$, at heat load 120W/m^2 were (1.0408, 1.0411, 1.0411, 1.0415, 1.0415, and 1.0418), at (X_1, X_2, X_3, X_4, X_5 , and X_6).
3. It was found that the values of temperature ratio of partially pilled carpet, always greater than full pilled carpet in all cases, this is because a hot partially pilled carpet is not completely covered with pile, unlike full pilled carpet, which is completely covered with pile, (pile) gives more resistance when heat is transferred through it, thus reducing the value of temperatures more for the air inside the room.
4. The partially pilled carpet has a greater impact on the room to be heated by using hot carpets
The partially pilled carpet has the highest temperature values and the lowest density values.

Availability of data and materials

The datasets generated during and/or analyzed during the current study are available from the corresponding author upon reasonable request.

Competing interests

The authors declare no competing interests.

Authors' contributions

All authors contributed to the study conception and design. Basem T.I. Ghobrial investigated the experimental data and prepared the original draft. Antar M.M. Abdala reviewed, edited and validated the results and manuscript. Khairy F.Megalla conceptualized and analyzed the results. Ahmed R abohabsa conceptualized and analyzed the results.

5. Acknowledgments

Not applicable

6. References

- [1] M. J. Varas-Muriel, R. Fort, and M. Gómez-Heras, "Assessment of an underfloor heating system in a restored chapel: Balancing thermal comfort and historic heritage conservation," *Energy Build.*, vol. 251, p. 111361, 2021, doi: 10.1016/j.enbuild.2021.111361.
- [2] H. Ikeda, Y. Ooi, and T. Nakaya, "Underfloor heating using room air conditioners with air source heat pump in a foundation insulation house," *Energies*, vol. 14, no. 21, pp. 1–29, 2021, doi: 10.3390/en14217034.
- [3] F. Hajabdollahi, Z. Hajabdollahi, and H. Hajabdollahi, "Thermo-economic modeling and optimization of underfloor heating using evolutionary algorithms," *Energy Build.*, vol. 47, pp. 91–97, 2012, doi: 10.1016/j.enbuild.2011.11.032.
- [4] A. Laafer, D. Semmar, A. Hamid, and M. Bourouis, "Thermal and surface radiosity analysis of an underfloor heating system in a bioclimatic habitat," *Energies*, vol. 14, no. 13, 2021, doi: 10.3390/en14133880.
- [5] A. Kankovsky and M. Dedic, "Wood flooring in combination with underfloor heating systems," *IOP Conf. Ser. Mater. Sci. Eng.*, vol. 1203, no. 2, p. 022043, 2021, doi: 10.1088/1757-899x/1203/2/022043.
- [6] M. S. Karimi, F. Fazelpour, M. A. Rosen, and M. Shams, "Comparative study of solar-powered underfloor heating system performance in distinctive climates," *Renew. Energy*, vol. 130, pp. 524–535, 2019, doi: 10.1016/j.renene.2018.06.074.
- [7] P. Devaux and M. M. Farid, "Benefits of PCM underfloor heating with PCM wallboards for space heating in winter," *Appl. Energy*, vol. 191,

- pp. 593–602, 2017, doi: 10.1016/j.apenergy.2017.01.060.
- [8] K. Faraj, J. Faraj, F. Hachem, H. Bazzi, M. Khaled, and C. Castelain, “Analysis of underfloor electrical heating system integrated with coconut oil-PCM plates,” *Appl. Therm. Eng.*, vol. 158, p. 113778, 2019, doi: 10.1016/j.applthermaleng.2019.113778.
- [9] G. Yu, Z. Lian, W. Gan, and J. Ji, “Numerical investigation on the effect of harmonic horizontal-axis rotation on laminar natural convection in an air-filled enclosure,” *Int. J. Heat Mass Transf.*, vol. 152, p. 119533, 2020, doi: 10.1016/j.ijheatmasstransfer.2020.119533.
- [10] J. D. Chung, H. Hong, and H. Yoo, “Analysis on the impact of mean radiant temperature for the thermal comfort of underfloor air distribution systems,” *Energy Build.*, vol. 42, no. 12, pp. 2353–2359, 2010, doi: 10.1016/j.enbuild.2010.07.030.
- [11] A. S. Krishnan, B. Premachandran, C. Balaji, and S. P. Venkateshan, “Combined experimental and numerical approaches to multi-mode heat transfer between vertical parallel plates,” *Exp. Therm. Fluid Sci.*, vol. 29, no. 1, pp. 75–86, 2004, doi: 10.1016/j.expthermflusci.2004.02.002.
- [12] M. Tye-Gingras and L. Gosselin, “Comfort and energy consumption of hydronic heating radiant ceilings and walls based on CFD analysis,” *Build. Environ.*, vol. 54, pp. 1–13, 2012, doi: 10.1016/j.buildenv.2012.01.019.
- [13] F. Hassan, H. Abdellatif, U. M. Rashed, and H. M. Ahmed, “Egyptian Journal of Chemistry,” vol. 78, no. 4, pp. 67–78, 2022, doi: 10.21608/EJCHEM.2021.98034.4574.
- [14] F. Saad, A. G. Hassabo, H. A. Othman, M. M. Mosaad, A. L. Mohamed, and T. Printing, “Egyptian Journal of Chemistry,” vol. 65, no. 4, pp. 431–448, 2022, doi: 10.21608/EJCHEM.2021.96612.4521.
- [15] M. Zayed, H. A. Othman, H. Ghazal, A. G. Hassabo, and T. Printing, “Egyptian Journal of Chemistry,” vol. 65, no. 4, pp. 499–524, 2022, doi: 10.21608/EJCHEM.2021.96598.4519.
- [16] M. A. Ali, E. A. Bydoon, and H. M. Ibrahim, “Egyptian Journal of Chemistry,” vol. 65, no. 4, pp. 525–542, 2022, doi: 10.21608/EJCHEM.2021.97103.4543.
- [17] S. A. Ebrahim, H. A. Othman, M. M. Mosaad, A. G. Hassabo, and T. Printing, “Egyptian Journal of Chemistry,” vol. 65, no. 4, pp. 555–568, 2022, doi: 10.21608/EJCHEM.2021.96717.4526.

Nomenclature		
I	electrical current	Amp.
Pr	Prandtl number	-
q	heat transfer rate	Watt
Ra	Rayleigh number	-
S	entropy	kJ/kg.K
T _{av}	average temperature	K
T _f	film temperature	K
T _{inf}	temperature of the air	K
Tr	temperature ratio	-
T _s	surface temperature	K
Y _r	height ratio	-
Greek symbols		
ζ	heating coefficient	-
ρ	density	kg/m ³
Subscript		
av	average	-
r	ratio	-
s	surface	-
inf	infinity	-
f	film	-
curr	current	-
Abbreviations and Acronyms		
EGM	entropy generation minimization	-
LMFBR	Liquid Metal Fast Breeder Reactor	-
RANS	Reynolds-Averaged Navier-Stokes	-
RH	Relative humidity	-